Anion−Macrodipole Interactions: Self-Assembling Oligourea/Amide Macrocycles as Anion Transporters that Respond to Membrane Polarization

ARTICLE *in* JOURNAL OF THE AMERICAN CHEMICAL SOCIETY · OCTOBER 2009

Impact Factor: 12.11 · DOI: 10.1021/ja9067518 · Source: PubMed

J|A|C|S
ARTICLES

Published on Web 10/30/2009

Anion−Macrodipole Interactions: Self-Assembling Oligourea/Amide Macrocycles as Anion Transporters that Respond to Membrane Polarization

Andreas Hennig,[†] Lucile Fischer,[‡] Gilles Guichard,*[,‡,§] and Stefan Matile*[,†]

Department of Organic Chemistry, University of Geneva, Geneva, Switzerland, and CNRS, Institut de Biologie Moléculaire et Cellulaire, Laboratoire d'Immunologie et Chimie Thérapeutiques, Strasbourg, France

Received August 10, 2009; E-mail: stefan.matile@unige.ch; g.guichard@ibmc.u-strasbg.fr

Abstract: Macrocyclic urea/amide hybrids are introduced as functional, anion-selective membrane transporters in lipid bilayer membranes. Six derivatives with varying side chains (aliphatic and aromatic) and conformations (parallel and antiparallel carbonyl dipoles) are investigated by fluorescence methods, among which the more active aromatic derivatives were selected for an in-depth study. Strong response of transport activity toward anion exchange and weak response toward cation exchange establish anion selectivity for all macrocycles. "Antiparallel" macrocycles that self-assemble into "antiparallel" nanotubes without macrodipole exhibit Hofmeister selectivity. Parallel macrocycles that self-assemble into parallel nanotubes with strong macrodipole are capable of overcoming the dehydration penalty of the Hofmeister bias. Both systems show additional chloride selectivity. The activity of antiparallel and parallel nanotubes in binary mixtures of bromide/perchlorate and chloride/thiocyanate is over- and underadditive, respectively (positive and negative AMFE). The activity of antiparallel nanotubes decreases rapidly with increasing membrane polarization, whereas parallel nanotubes are inactivated at high and activated by membrane potentials at low concentration. Hill coefficients of parallel nanotubes decrease significantly with membrane polarization, whereas those of antiparallel nanotubes increase slightly. The overall unusual characteristics of parallel nanotubes call for a new transport mechanism, where macrodipole−potential interactions account for voltage sensitivity and anion−macrodipole interactions account for anion selectivity.

Introduction

The synthesis, design, and characterization of novel structures for anion transport across lipid bilayer membranes has received much attention during recent years because of its importance for understanding biological anion transport and its potential regarding the development of anion sensors, anion-selective electrodes, and antimicrobials.[1−4] Therefore, numerous biomimetic approaches toward anion transport have so far been envisaged on the basis of the modification of natural occurring motifs from proteins,[5−7] antimicrobial peptides,[8,9] and natural products.[10−16] Further inspiration from the development of anion receptors[17] and sensors[18] has stimulated the field to create functional systems that exploit the use of potent hydrogen-bond donors,[19−27] ion pairing motifs,[8−13,27−29] catechols,[30] and anion−π interactions.[31−34]

An additional favorable interaction, which has become prominent in structural biology, is exerted by the macrodipole of α-helical peptides and protein subunits on ionic species.[35,36]

[†] University of Geneva.
[‡] CNRS Strasbourg.
[§] Present address: Institut Européen de Chimie et Biologie, Université de Bordeaux-CNRS UMR 5248, 2 rue Robert Escarpit, 33607 Pessac, France.

(1) Davis, A. P.; Sheppard, D. N.; Smith, B. D. *Chem. Soc. Rev.* **2007**, *36*, 348–357.
(2) Gokel, G. W.; Barkey, N. *New J. Chem.* **2009**, *33*, 348–357.
(3) Sisson, A. L.; Shah, M. R.; Bhosale, S.; Matile, S. *Chem. Soc. Rev.* **2006**, *35*, 1269–1286.
(4) Matile, S.; Som, A.; Sordé, N. *Tetrahedron* **2004**, *60*, 6405–6435.
(5) Broughman, J. R.; Shank, L. P.; Takeguchi, W.; Schultz, B. D.; Iwamoto, T.; Mitchell, K. E.; Tomich, J. M. *Biochemistry* **2002**, *41*, 7350–7358.
(6) Suzuki, M.; Morita, T.; Iwamoto, T. *Cell. Mol. Life Sci.* **2006**, *63*, 12–24.
(7) Pajewski, R.; Ferdani, R.; Pajewska, J.; Djedovi, N.; Schlesinger, P. H.; Gokel, G. W. *Org. Biomol. Chem.* **2005**, *3*, 619–625.
(8) Patch, J. A.; Barron, A. E. *J. Am. Chem. Soc.* **2003**, *125*, 12092–12093.
(9) Epand, R. F.; Raguse, T. L.; Gellman, S. H.; Epand, R. M. *Biochemistry* **2004**, *43*, 9527–9535.
(10) Deng, G.; Dewa, T.; Regen, S. L. *J. Am. Chem. Soc.* **1996**, *118*, 8975–8976.
(11) Merritt, M.; Lanier, M.; Deng, G.; Regen, S. L. *J. Am. Chem. Soc.* **1998**, *120*, 8494–8501.
(12) Otto, S.; Osifchin, M.; Regen, S. L. *J. Am. Chem. Soc.* **1999**, *121*, 7276–7277.
(13) Jiang, C.; Lee, E. R.; Lane, M. B.; Xiao, Y.-F.; Harris, D. J.; Cheng, S. H. *Am. J. Physiol.* **2001**, *281*, L1164.
(14) Ding, B.; Yin, N.; Liu, Y.; Cardenas-Garcia, J.; Evanson, R.; Orsak, T.; Fan, M.; Turin, G.; Savage, P. B. *J. Am. Chem. Soc.* **2004**, *126*, 13642–13648.
(15) Ilker, M. F.; Nusslein, K.; Tew, G. N.; Coughlin, E. B. *J. Am. Chem. Soc.* **2004**, *126*, 15870–15875.
(16) Sessler, J. L.; Eller, L. R.; Cho, W.-S.; Nicolaou, S.; Aguilar, A.; Lee, J. T.; Lynch, V. M.; Magda, D. J. *Angew. Chem., Int. Ed.* **2005**, *44*, 5989–5992.
(17) Gale, P. A. *Acc. Chem. Res.* **2006**, *39*, 465–475.
(18) Davis, J. T.; Gale, P. A.; Okunola, O. A.; Prados, P.; Iglesias-Sánchez, J. C.; Torroba, T.; Quesada, R. *Nat. Chem.* **2009**, *1*, 138–144.
(19) Caltagirone, C.; Gale, P. A. *Chem. Soc. Rev.* **2009**, *38*, 520–563.
(20) Martinez-Manez, R.; Sancenon, F. *Chem. Rev.* **2003**, *103*, 4419–4476.

This kind of interaction has been held responsible for the selectivity of potassium, chloride, and water channels,[37−39] variations of amino acid pK_a values in model peptides,[40] nucleation of helix formation,[41,42] and significant contributions toward anion binding by proteins.[43−45] Despite its vast importance in natural biological systems, macrodipolar interactions in general and anion−macrodipole interactions in particular have so far only been poorly applied in chemical or biomimetic functional systems.[46]

The self-assembly of urea-based and amide-based peptidomimetic macrocycles into nanotubes and their ability to bind anions has been studied extensively.[47−57] Furthermore, numerous applications in catalysis, biotechnology, and materials science have been envisaged.[47−57] The self-assembly of cyclic D,L-α-peptides into nanotubes has been used to produce artificial ion channels in several variations.[49−51] The antiparallel alignment of amide functionalities in these nanotubes is thought to account for the voltage independence of the obtained cation-selective channels.[49] The parallel alignment of carbonyl groups in cyclic β^3-peptides has been proposed to give nanotubes with strong macrodipoles.[50] The functional consequences of the proposed macrodipole in β^3-peptide ion channels have not been investigated.[50]

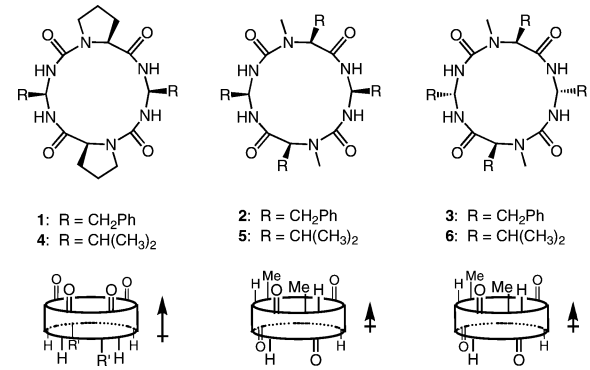

Figure 1. Structures of oligourea/amide macrocycles **1**−**6** with aryl (**1**−**3**) and alkyl (**4**−**6**) side chains with schematic conformers derived from X-ray and NMR.[57] Arrows indicate molecular dipoles; conformers with antiparallel carbonyls preserve a small molecular dipole because the dipole moment of ureas exceeds that of amides.[58]

In this Article, we investigate the transport activity of peptidomimetic oligourea/amide macrocycles **1**−**6** (Figure 1). The structural aspects of **1**, **4**, and **5** have been characterized in detail by NMR and X-ray analysis and were recently reported.[57] In brief, **5** and a related isobutyl-derivative formed N−H···O═C hydrogen-bonded antiparallel dimers in solution, which self-assembled in the solid state into tubular stacks through additional weak interactions. In contrast, **1** and **4** formed parallel tubular stacks in the solid state and in solution. The parallel nanotube formed by **1** contains one bridging water molecule between each macrocycle. Accepting two H-bonds from one macrocycle and donating two to the other, these bridging water molecules are uniformly oriented to further increase the macrodipole of the parallel nanotube. Oligourea/amide macrocycles that self-assemble into antiparallel and parallel nanotubes with similar global structure appeared ideal to explore the importance of macrodipoles for anion binding, anion transport, and voltage gating.

Results

Activity. The transport activity of **1**−**6** was assessed with the HPTS assay.[32,59,60] For this purpose, large unilamellar vesicles (LUV) were prepared from egg yolk phosphatidylcholine

(21) Sidorov, V.; Kotch, F. W.; Abdrakhmanova, G.; Mizani, R.; Fettinger, J. C.; Davis, J. T. *J. Am. Chem. Soc.* **2002**, *124*, 2267–2278.
(22) Santacroce, P. V.; Okunola, O. A.; Zavalij, P. Y.; Davis, J. T. *Chem. Commun.* **2006**, 3246–3248.
(23) McNally, B. A.; Koulov, A. V.; Smith, B. D.; Joos, J.-B.; Davis, A. P. *Chem. Commun.* **2005**, 1087–1089.
(24) Clare, J. P.; Ayling, A. J.; Joos, J.-B.; Sisson, A. L.; Magro, G.; Perez-Payan, M. N.; Lambert, T. N.; Shukla, R.; Smith, B. D.; Davis, A. P. *J. Am. Chem. Soc.* **2005**, *127*, 10739–10746.
(25) McNally, B. A.; O'Neil, E. J.; Nguyen, A.; Smith, B. D. *J. Am. Chem. Soc.* **2008**, *130*, 17274–17275.
(26) Li, X.; Wu, Y.-D.; Yang, D. *Acc. Chem. Res.* **2008**, *41*, 1428–1438.
(27) Madhavan, N.; Robert, E. C.; Gin, M. S. *Angew. Chem., Int. Ed.* **2005**, *44*, 7584–7587.
(28) Izzo, I.; Licen, S.; Maulucci, N.; Autore, G.; Marzocco, S.; Tecilla, P.; De Riccardis, F. *Chem. Commun.* **2008**, 2986–2988.
(29) Licen, S.; Coppola, C.; D'Onofrio, J.; Montesarchio, D.; Tecilla, P. *Org. Biomol. Chem.* **2009**, *7*, 1060–1063.
(30) Berezin, S. K.; Davis, J. T. *J. Am. Chem. Soc.* **2009**, *131*, 2458–2459.
(31) Gorteau, V.; Bollot, G.; Mareda, J.; Perez-Velasco, A.; Matile, S. *J. Am. Chem. Soc.* **2006**, *128*, 14788–14789.
(32) Gorteau, V.; Bollot, G.; Mareda, J.; Matile, S. *Org. Biomol. Chem.* **2007**, *5*, 3000–3012.
(33) Perez-Velasco, A.; Gorteau, V.; Matile, S. *Angew. Chem., Int. Ed.* **2008**, *47*, 921–923.
(34) Mareda, J.; Matile, S. *Chem.-Eur. J.* **2009**, *15*, 28–37.
(35) Hol, W. G. J.; van Duijnen, P. T.; Berendsen, H. J. C. *Nature* **1978**, *273*, 443–446.
(36) Hol, W. G. J. *Adv. Biophys.* **1985**, *19*, 133–165.
(37) Doyle, D. A.; Morais Cabral, J.; Pfuetzner, R. A.; Kuo, A.; Gulbis, J. M.; Cohen, S. L.; Chait, B. T.; MacKinnon, R. *Science* **1998**, *280*, 69–77.
(38) Dutzler, R.; Campbell, E. B.; MacKinnon, R. *Science* **2003**, *300*, 108–112.
(39) de Groot, B. L.; Grubmüller, H. *Curr. Opin. Chem. Biol.* **2005**, *15*, 176–183.
(40) Joshi, H. V.; Meier, M. S. *J. Am. Chem. Soc.* **1996**, *118*, 12038–12044.
(41) Hudgins, R. R.; Jarrold, M. F. *J. Am. Chem. Soc.* **1999**, *121*, 3494–3501.
(42) Hart, S. A.; Bahadoor, A. B. F.; Matthews, E. E.; Qiu, X. J.; Schepartz, A. *J. Am. Chem. Soc.* **2003**, *125*, 4022–4023.
(43) Wang, H.; McIntosh, L. P.; Graves, B. J. *J. Biol. Chem.* **2002**, *277*, 2225–2233.
(44) Faraldo-Gómez, J. D.; Roux, B. *J. Mol. Biol.* **2004**, *339*, 981–1000.
(45) Hirsch, A. K.; Fischer, F. R.; Diederich, F. *Angew. Chem., Int. Ed.* **2007**, *46*, 338–352.
(46) Kimura, S. *Org. Biomol. Chem.* **2008**, *6*, 1143–1148.
(47) Benedetti, E.; DiBlasio, B.; Pedone, C.; Lorenzi, G. P.; Tomasic, L.; Gramlich, V. *Nature* **1979**, *282*, 630.
(48) Ranganathan, D.; Lakshmi, C.; Karle, I. L. *J. Am. Chem. Soc.* **1999**, *121*, 6103–6107.
(49) Bong, D. T.; Clark, T. D.; Granja, J. R.; Ghadiri, M. R. *Angew. Chem., Int. Ed.* **2001**, *40*, 988–1011.
(50) Clark, T. D.; Buehler, L. K.; Ghadiri, M. R. *J. Am. Chem. Soc.* **1998**, *120*, 651–656.
(51) Wang, D.; Guo, L.; Zhang, J.; Jones, L. R.; Chen, Z.; Pritchard, C.; Roeske, R. W. C. *J. Pept. Res.* **2001**, *57*, 301–306.
(52) Seebach, D.; Matthews, J. L.; Meden, A.; Wessels, T.; Baerlocher, C.; McCusker, L. B. *Helv. Chim. Acta* **1997**, *80*, 173–182.
(53) Yang, J.; Dewal, M. B.; Profeta, S.; Smith, M. D.; Li, Y.; Shimizu, L. S. *J. Am. Chem. Soc.* **2008**, *130*, 612–621.
(54) Brea, R. J.; Vazquez, M. E.; Mosquera, M.; Castedo, L.; Granja, J. R. *J. Am. Chem. Soc.* **2007**, *129*, 1653–1657.
(55) Meshcheryakov, D.; Böhmer, V.; Bolte, M.; Hubscher-Bruder, V.; Arnaud-Neu, F.; Herschbach, H.; Van Dorsselaer, A.; Thondorf, I.; Mögelin, W. *Angew. Chem., Int. Ed.* **2006**, *45*, 1648–1652.
(56) Semetey, V.; Didierjean, C.; Briand, J. P.; Aubry, A.; Guichard, G. *Angew. Chem., Int. Ed.* **2002**, *41*, 1895–1898.
(57) Fischer, L.; Decossas, M.; Briand, J.-P.; Didierjean, C.; Guichard, G. *Angew. Chem., Int. Ed.* **2009**, *48*, 1625–1628.
(58) Lide, D. R. *CRC Handbook of Chemistry and Physics*, 85th ed.; CRC Press: New York, 2004.
(59) Sakai, N.; Matile, S. *J. Phys. Org. Chem.* **2006**, *19*, 452–460.
(60) Matile, S.; Sakai, N. The Characterization of Synthetic Ion Channels and Pores. In *Analytical Methods in Supramolecular Chemistry*; Schalley, C., Ed.; Wiley: Weinheim, 2007; pp 391−418.

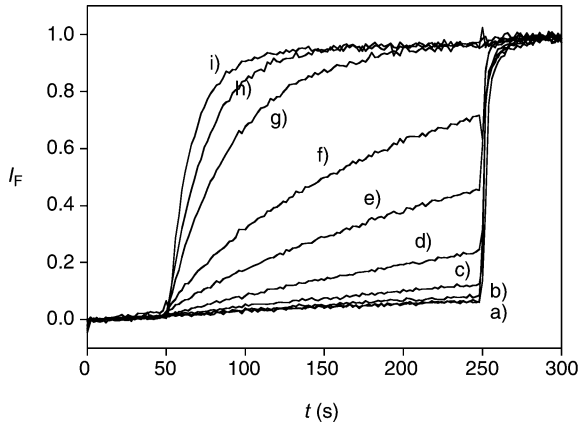

Figure 2. Changes in ratiometric fluorescence intensity I_F of HPTS ($\lambda_{ex,1}$ = 405 nm, $\lambda_{ex,2}$ = 450 nm, λ_{em} = 510 nm) during addition of **3** ((a) 10 nM, (b) 30 nM, (c) 100 nM, (d) 300 nM, (e) 1 μM, (f) 3 μM, (g) 5 μM, (h) 10 μM, and (i) 30 μM final concentration) at 50 s to EYPC-LUVs ⊃ HPTS with ΔpH ≈ 0.8 (~32 μM EYPC). Fluorescence ratiometric changes were subtracted from the initial intensity and normalized to the final intensity after addition of 1 μM gramicidin A at 250 s.

(EYPC), loaded with the pH-sensitive fluorescent dye 8-hydroxy-1,3,6-pyrenetrisulfonate (HPTS), and exposed to a pH gradient (ΔpH = 0.8) across the vesicle membrane. The addition of **1**−**6** to these vesicles led to ratiometric changes in HPTS emission (Figures 2, S1, and S2).[59,60] The excitation maximum at 405 nm decreases with pH, whereas that at 450 nm increases. Comparison of double channel kinetics recorded at the two maxima can thus reveal changes in pH without any interference from unrelated effects. The observed changes in ratiometric HPTS emission report on the change in local pH in response to sample addition, a change that can occur by facilitated H^+/M^+ antiport, OH^-/X^- antiport, H^+/X^- symport, OH^-/M^+ symport, HPTS export, or vesicle destruction.[60] In this assay, activities are quantified with EC_{50} and n values, which are both obtained from dose response curves. Hill coefficients $n > 1$ demonstrate the presence of unstable supramolecules that exist as minority component besides an excess of inactive monomers and act cooperatively.[61−63] Hill coefficients $n \leq 1$ demonstrate that the active structure is either a monomer or a stable supramolecule. The EC_{50} is the "effective" concentration, that is, the concentration of monomers needed to observe 50% activity. Because delivery, partitioning, and self-organization or self-assembly are never quantitative, EC_{50}'s are always overestimates. With $n >$ 1 systems, the real concentration of the unstable active supramolecule is by definition much lower (at least 1 order of magnitude, usually much more).

According to the HPTS assay, alkyl-substituted macrocycles **4**−**6** had EC_{50}'s > 60 μM (Figure S1). The activities of aryl-substituted macrocycles **1**−**3** were with EC_{50}'s = 1.9−4.3 μM at least 1 order of magnitude better (Figures 2 and S2). Extensive precedence in the literature suggested that this difference originates from preferred partitioning and translocation of aromatic as compared to aliphatic compounds.[65−69] The relative activities within the aryl and alkyl series were quite similar. Control experiments with internally added *p*-xylene-bis-pyridinium bromide (DPX) as a quencher of HPTS fluorescence under otherwise identical conditions showed no transport activity, thus confirming the absence of partial lysis or unselective leaks in the bilayer membrane (Figure S3).

Selectivity. Extravesicular anion and cation exchange is routinely used to differentiate between anion and cation transport with the HPTS assay.[59,60] With macrocycles **1**−**3**, external anion exchange caused much stronger changes than did external cation exchange (Figure 3A and B). Responsiveness to external anion exchange suggested that macrocycles **1**−**3** preferably transport anions. The observed anion selectivities of **2** and **3** were very similar and followed the Hofmeister series (Figure 3C). This suggested that transport activity is dominated by the dehydration penalty of transferring an anion into the lipid bilayer and not by anion binding to the macrocycles **2** or **3**.

The anion selectivity of macrocycle **1** followed the opposite trend (Figure 3D). The found "anti-Hofmeister" selectivity implied that transport by macrocycle **1** is dominated by binding to the active suprastructure. Both "anti-Hofmeister" macrocycle **1** and "Hofmeister" macrocycle **2** showed extra selectivity for chloride. These high activities with external chloride were observed not only in the presence of internal chloride but also in the presence of internal bromide (Figure 3Ac, solid vs dotted line). The general insensitivity toward internal Cl^-/Br^- exchange further suggested that transmembrane X^-/Cl^- or X^-/Br^- exchange is intrinsically faster and thus preceding the OH^- or H^+ transport reported by HPTS. These differences were as expected because of the, as compared to OH^-/H^+, much higher $X^-/Cl^-/Br^-$ concentrations involved, and not because of any selectivity.[32]

Anomalous Mole Fraction Effect (AMFE). The dependence of transport activity of macrocycles **1** and **2** on the mole fraction of binary mixtures of anions was determined next using the HPTS assay. Of particular interest were mixtures of "fast" and "slow" anions, that is, anions that cause high transport activity in the HPTS assay combined with anions that cause low transport activity in the HPTS assay. For the "Hofmeister-type" macrocycle **2**, the fast perchlorate was combined with the slow bromide (Figure 4B) and the fast SCN^- was combined with the slower Cl^- (Figure 4D). The "anti-Hofmeister" selectivity of the macrocycle **1** reversed these situations to fast Br^- being combined with slow perchlorates (Figure 4A), and fast Cl^- being combined with the slower SCN^- (Figure 4C).

The dependence of transport activity of macrocycles **1** and **2** on the mole fraction of these binary mixtures of fast and slow anions differed from linear additivity. With macrocycle **2**, overadditivity or a positive anomalous mole fraction effect (AMFE) was found. Saturation behavior with the fast anion can conceivably account for these positive AMFEs.

The underadditivity or negative AMFE found with macrocycle **1** was more interesting. Negative AMFE is often observed

(61) Litvinchuk, S.; Bollot, G.; Mareda, J.; Som, A.; Ronan, D.; Shah, M. R.; Perrottet, P.; Sakai, N.; Matile, S. *J. Am. Chem. Soc.* **2004**, *126*, 10067–10075.
(62) Bhosale, S.; Matile, S. *Chirality* **2006**, *18*, 849–856.
(63) Mora, F.; Tran, D.-H.; Oudry, N.; Hopfgartner, G.; Jeannerat, D.; Sakai, N.; Matile, S. *Chem.-Eur. J.* **2008**, *14*, 1947–1953.
(64) Yau, W. M.; Wimley, W. C.; Gawrisch, K.; White, S. H. *Biochemistry* **1998**, *37*, 14713–14718.
(65) Babakhani, A.; Gorfe, A. A.; Kim, J. E.; McCammon, J. A. *J. Phys. Chem. B* **2008**, *112*, 10528–10534.
(66) Sanderson, J. M.; Whelan, E. J. *Phys. Chem. Chem. Phys.* **2004**, *6*, 1012–1017.
(67) De Planque, M. R. R.; Bonev, B. B.; Demmers, J. A. A.; Greathouse, D. V.; Koeppe, R. E., II; Separovic, F.; Watts, A.; Killian, J. A. *Biochemistry* **2003**, *42*, 5341–5348.
(68) Perret, F.; Nishihara, M.; Takeuchi, T.; Futaki, S.; Lazar, A. N.; Coleman, A. W.; Sakai, N.; Matile, S. *J. Am. Chem. Soc.* **2005**, *127*, 1114–1115.
(69) Nishihara, M.; Perret, F.; Takeuchi, T.; Futaki, S.; Lazar, A. N.; Coleman, A. W.; Sakai, N.; Matile, S. *Org. Biomol. Chem.* **2005**, *3*, 1659–1669.

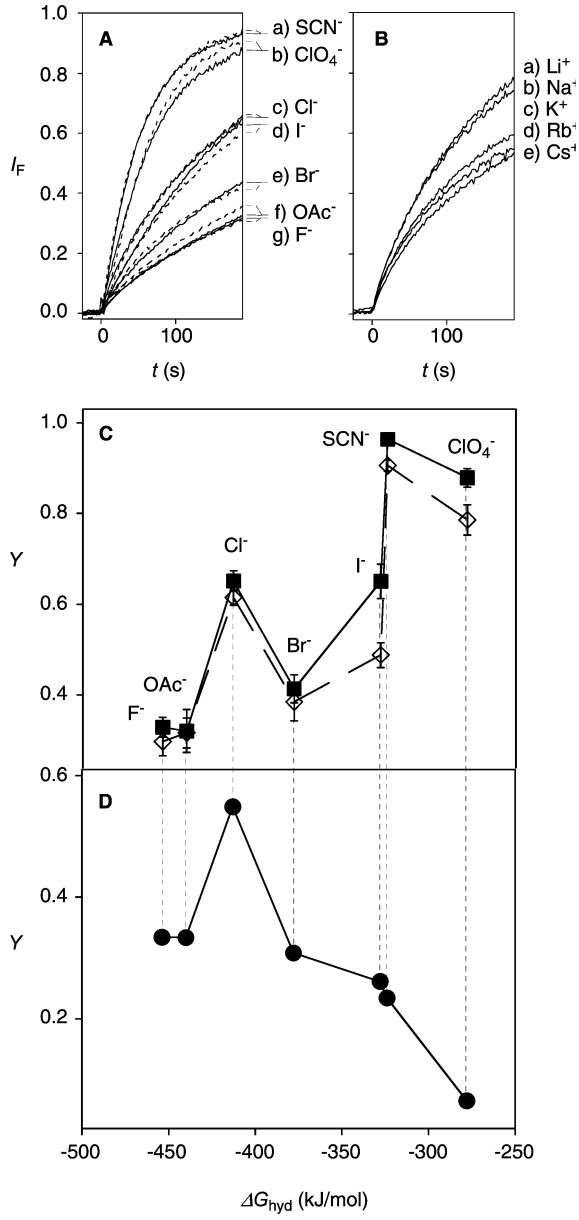

Figure 3. Anion/cation selectivity (A,B) and anion selectivity topology of macrocycles **1** (●), **2** (A−C, ■), and **3** (◇). (A,B) HPTS emission after addition of **1**−**3** (constant concentration) to EYPC-LUVs ⊃ HPTS with $\Delta pH \approx 0.8$, internal NaX (X = Cl (solid), Br (dotted)) and external NaX (A) or MCl (B), M and X as indicated. (C,D) Fractional activity *Y* as a function of the anion hydration energies (in part from (A) and (B)).

with biological ion channels,[70] and its explanation commonly refers to a cooperative multiion transport process.[71−74]

Voltage Gating. The dependence of transport activity of macrocycles **1** and **2** on the membrane potential was determined in doubly labeled vesicles with internal HPTS as pH sensitive and external safranin O as potential sensitive fluorescent probe.[75−79] To apply inside negative membrane potentials,

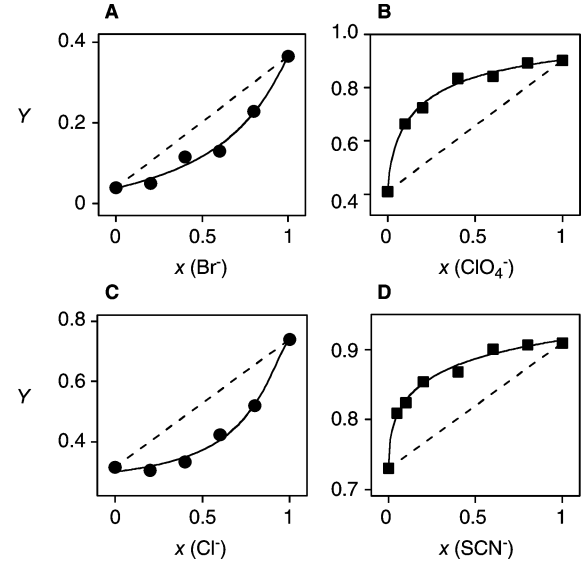

Figure 4. Dependence of fractional activity of **1** (●) and **2** (■) on the mole fraction *x* of mixtures of Br^- and ClO_4^- (A,B) and mixtures of Cl^- and SCN^- (C,D). The total salt concentration was 100 mM for all combinations.

vesicles were loaded with K^+, osmotically counterbalanced with external Na^+, and treated with the K^+ carrier valinomycin. Application of membrane potential with valinomycin and pH gradient with base was recorded in triple-channel kinetics with external safranin O ($\lambda_{exc} = 522$ nm, $\lambda_{em} = 581$ nm, Figure 5B) and internal HPTS (Figure 5A), respectively.[60,75−79]

According to this modified HPTS assay in polarized vesicles, the activity of macrocycles **1**−**3** decreased with increasing membrane polarization (Figure 5A, empty symbols vs filled symbols). The concomitant changes in membrane potential caused by macrocycle **3** (Figure 5B, red ◆) and particularly macrocycle **1** (Figure 5A, blue ●) were nearly negligible. These results confirmed the high anion selectivity found in external ion exchange experiments. Particularly for macrocycle **1**, they further suggested that anion selectivity is fully retained at high membrane polarization.

The dependence of the activity of macrocycles **1**−**3** on membrane polarization was summarized in formal *I*−*V* profiles (Figure 5C−E). Macrocycles **2** (Figure 5D) and **3** (Figure 5E) responded similarly with a steep decrease in activity upon inside negative polarization. At high potentials, the activity of **2** recovered (Figure 5D), an effect that was accompanied by increasing membrane depolarization and thus presumably due to a loss in selectivity and/or change in mechanism of transport (Figure 5B, black ■).

Gating charges $z_g = 0.54 \pm 0.08$ and $z_g = 0.56 \pm 0.05$ were calculated from exponential curve fit for **2** and **3**. These significant voltage dependences were in the range of synthetic ion channels ($z_g = 0.85$) or the bee toxin melittin ($z_g = 1.50$).[78] With $z_g = 0.14 \pm 0.01$, macrocycle **1** was clearly less voltage sensitive under the selected conditions (Figure 5C).

To determine the dependence of the voltage sensitivity on the concentration of macrocycles **1** and **2**, Hill plots were measured at 0 and −160 mV. The concentration dependence[60−64]

(70) Hille, B.; Schwarz, W. *J. Gen. Physiol.* **1978**, *72*, 409–442.
(71) Nonner, W.; Chen, D. P.; Eisenberg, B. *Biophys. J.* **1998**, *74*, 2327–2334.
(72) Miller, C. *J. Gen. Physiol.* **1999**, *113*, 783–787.
(73) Qu, Z.; Hartzell, H. C. *J. Gen. Physiol.* **2000**, *116*, 825–844.
(74) Gillespie, D.; Boda, D.; He, Y.; Apel, P.; Siwy, Z. S. *Biophys. J.* **2008**, *95*, 609–619.
(75) Sakai, N.; Matile, S. *Chem.-Eur. J.* **2000**, *6*, 1731–1737.
(76) Sakai, N.; Gerard, D.; Matile, S. *J. Am. Chem. Soc.* **2001**, *123*, 2517–2524.
(77) Sakai, N.; Matile, S. *J. Am. Chem. Soc.* **2002**, *124*, 1184–1185.
(78) Sakai, N.; Houdebert, D.; Matile, S. *Chem.-Eur. J.* **2003**, *9*, 223–232.
(79) Sakai, N.; Matile, S. *Chem. Biodiversity* **2004**, *1*, 28–43.

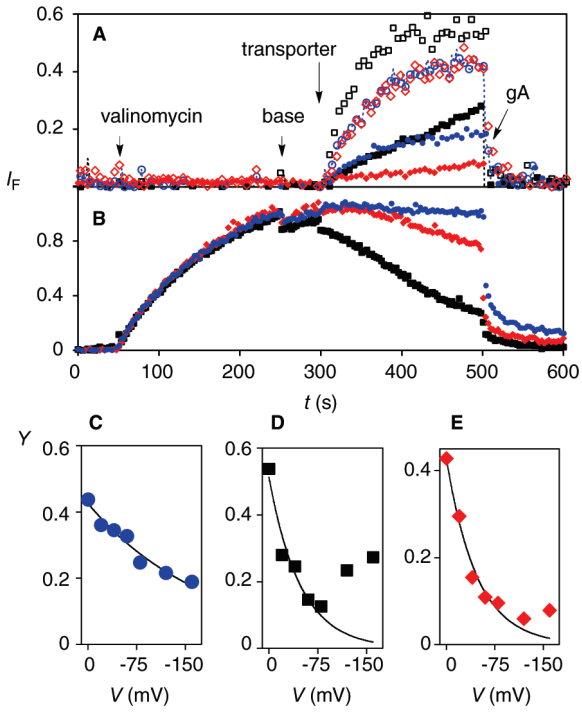

Figure 5. Voltage dependence of **1** (○, ●, 3 μM), **2** (□, ■, 3 μM), and **3** (◇, ◆, 2 μM). Changes in I_F of HPTS (A) and safranin O (B) after addition of valinomycin (1 μM, t = 50 s), NaOH (5 mM, t = 250 s), and **1** (○, ●), **2** (□, ■), and **3** (◇, ◆) to K^+-loaded (100 mM) LUVs. Representative traces with 100 mM (0 mV, ○, □, ◇) and 0.2 mM (−160 mV, ●, ■, ◆) external K^+ are shown. (C−E) Dependence of the fractional activity Y on the applied membrane potential for **1** (C), **2** (D), and **3** (E).

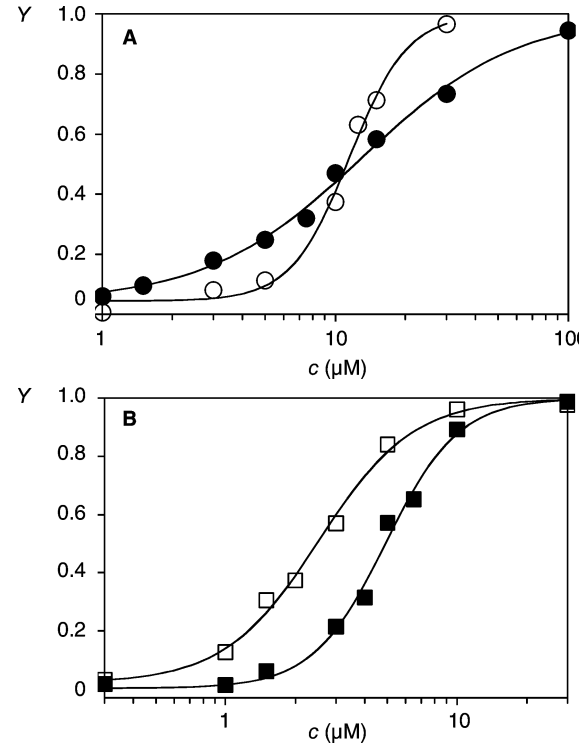

Figure 6. Dependence of the fractional activity on the concentration of **1** (A) and **2** (B) with external Br^- at −160 mV (filled symbols) and 0 mV (empty symbols).

of macrocycle **2** revealed that membrane polarization results in an increased EC_{50} (i.e., effective concentration needed to reach 50% activity) at a slightly increasing Hill coefficient n (Figure 6B). The Hill plot of macrocycle **1** revealed the opposite behavior. Membrane polarization caused a strong decrease of the Hill coefficient from $n = 4$ at $V = 0$ mV to $n = 1$ at $V = -160$ mV, whereas the EC_{50} did not change much (Figure 6A). This unusual behavior demonstrated that the voltage gating of macrocycle **1** is concentration dependent. At concentrations above the EC_{50}, membrane polarization causes the inactivation of macrocycle **1**, whereas voltage-gated activation is observed below the EC_{50}.

Strongly decreasing Hill coefficients with increasing membrane potentials were reproducibly observed for macrocycle **1** in the presence of external F^-, Cl^-, and Br^- and internal Cl^- (Figure S10). The complementary weak increase of Hill coefficients with increasing membrane potentials was reproducibly observable for macrocycle **2** under the same conditions. The dependence of the EC_{50} on membrane polarization in the presence of different external anions was both less significant and more complex, influenced, for example, by the impact of membrane potentials on anion binding at the membrane−water interfaces, and so on.

Flip Flop. For mechanistic considerations, the ability of macrocycles **1**−**3** to facilitate transversal diffusion (flip−flop) of phospholipids was evaluated as well.[80,81] For this purpose, EYPC-LUVs were doped with 0.25% NBD-DPPE (7-nitrobenz-2-oxa-1,3-diazol-4-yl-dipalmitoylphosphatidyl-ethanolamine). Reduction of the outside NBD by dithionite and subsequent purification by size exclusion chromatography gave inside labeled vesicles. After incubation with macrocycles **1**−**3** for different periods of time, sodium dithionite was added, and the reduction in fluorescence was recorded. The inability of macrocycles **1**−**3** to transport dithionite efficiently suggested that this reduction in fluorescence indicates the extent of transversal diffusion of NBD-PE. A clear dependence of the reduction in fluorescence on incubation time suggested that macrocycles **1**−**3** have flippase activity (Figure S12). The observed flippase activity was weak, much weaker than the flippase activities of micellar or toroidal pores[81] or synthetic flippases,[80] and thus in agreement with a "Jacobs-ladder" mechanism introduced in the following.

Discussion

The ability of oligourea/amide macrocycles **1**−**3** to transport ions across bilayer membranes as such did not come as a surprise. The question rather was if the found characteristics are novel and significant. To demonstrate significance, biphasic or dichotomic behavior is ideal. The dichotomy found for macrocycles **1** and **2** is stunning. Macrocycle **2** shows Hofmeister selectivity, positive AMFE, and biphasic but concentration-independent voltage dependence with increasing EC_{50} and constant n. Macrocycle **1** shows strictly the contrary (i.e., anti-Hofmeister selectivity, negative AMFE and exponential, but concentration-dependent voltage dependence with increasing n and constant EC_{50}). This dichotomic behavior was ideal to demonstrate significance because isolate trends in complex systems can originate from less or completely unrelated processes. The response of **1** alone to different anions or membrane polarization, for example, could possibly originate from changes in partitioning or even from simply overlooked

(80) Smith, B. D.; Lambert, T. N. *Chem. Commun.* **2003**, 2261–2268.
(81) Matsuzaki, K.; Murase, O.; Fujii, N.; Miyajima, K. *Biochemistry* **1996**, *35*, 11361–11368.

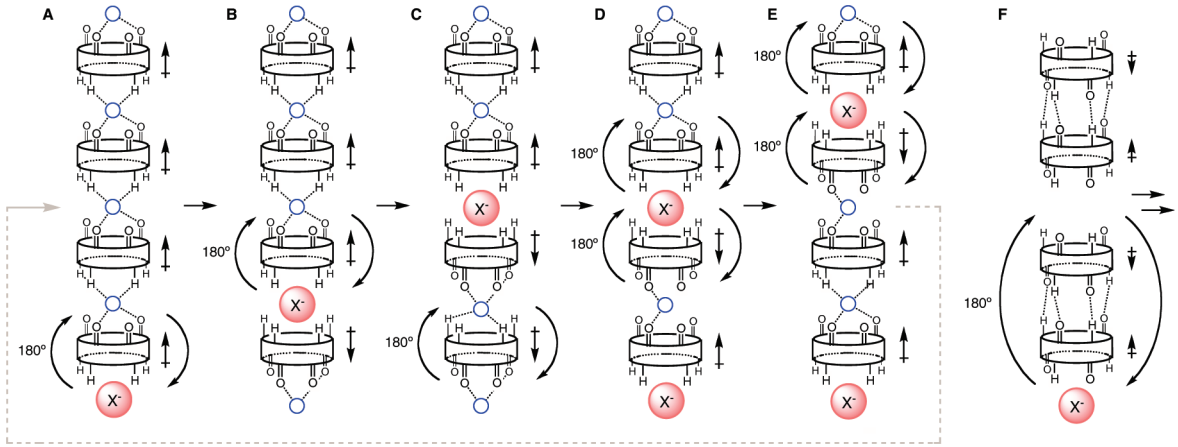

Figure 7. A tentative and simplified "Jacobs-ladder" mechanism for the transport of anions X^- by macrocycles **1** (A−E) and **2** (F). Blue circles stand for water (or occasional H_3O^+); see text for details.

technical errors. Direct determination of the impact of partitioning, etc., on apparent ion selectivity, voltage dependence, etc., is not possible because in $n > 1$ systems, the active minority is obscured by an inactive majority (see above).[61−63] However, dichotomic response of **2** under the same conditions demonstrated that at least one of the two opposing trends found for **1** and **2** is significant.

Biphasic behavior proves significance for similar reasons. A less related process such as delivery or partitioning could account for either the decreasing activity of **2** at low or the increasing activity at high membrane potential, but not for both phenomena (Figure 5D). The same holds for voltage-gated activation of **1** at low and inactivation at high concentration (Figure 6A), and so on. Validity of this interpretation was corroborated by the dichotomic nature of both processes (Figures 5C and 6B).

As far as novelty was concerned, the intriguing profile of macrocycle **1** contrasted sharply from the mainstream characteristics of the dichotomic macrocycle **2** (except for biphasic voltage dependence). The following discussion will thus focus on the significant macrocycle **1** and mention the dichotomic macrocycle **2** for comparison and completion only.

Mechanism. On first view, the crystal structure of macrocycle **1** might suggest that anion transport through the "parallel" nanotube formed by the stacked macrocycles would account for the intriguing properties of this system.[57] However, closer inspection revealed that anions are far too big for inclusion within and transport through the nanotube (diameter of $F^- = 2.7$ Å, inner nanotube diameter ≤ 1.8 Å).[57] Only dehydrated lithium would fit ($d = 1.52$ Å), an observation that could explain the high activity observed in the presence of this cation (Figure S4).

Selective anion transport through larger pores between four tubes aligned in a barrel-stave fashion[3,4] as seen in the solid state[57] was similarly unlikely. These flexible pores should not exclude molecules such as DPX or HPTS (Figure S3), and their π-basic interior should select for cations rather than for anions (Figure 3).[31−34] Anion selectivity and inability to transport larger anions and cations thus suggested that in lipid bilayers, the hydrophobic nanotubes formed by **1** do not further self-assemble in porous bundles. The possibility that macrocycle **1** acts as monomeric anion carrier was very unlikely for several reasons, including Hill coefficients $n > 1$.

The intriguing behavior of macrocycle **1** thus ruled out presently accepted mechanisms. Remarkably well imitating the historical "Jacobs-ladder" toy, the transport mechanism proposed in the following will be referred to as the "Jacobs-ladder" mechanism (Figure 7). In this mechanism, macrocycles **1** self-assemble into water-bridged parallel nanotubes known from the solid state.[57] Attracted by their macrodipole, anions bind to the four hydrogen-bond donors at the positive end of the macrodipole (Figure 7A). Rotation of the first macrocycle by 180° allows the anion to enter the nanotube (Figure 7B). In this process, the loss in macrodipole and water-mediated H-bonding between the macrocycles in the thermodynamically unstable active suprastructure (see below) is overcompensated by anion binding to eight preorganized hydrogen-bond donors from two antiparallel macrocycles. Continuing rotation of the subsequent macrocycles should allow single anions to move on to the other side of the membrane in a multiequilibrium process that leads to a full inversion of the macrodipole (Figure 7A−C).

Consideration of a cooperative multiion process is required to explain directional transport without macrodipole inversion. Driven by a transmembrane anion gradient, macrocycle can rotate to take up another anion that in turn repels the first one toward the other side and restores the macrodipole (Figure 7D,E). In a pentameric tube, binding of maximal three anions at the same time would be conceivable. To maintain transmembrane charge neutrality, not only anion antiport but also anion−proton or anion−cation symport by protonation of a bridging water[57] or its exchange with a cation appear all possible (lithium would be preferable in this case because it could also move through the nanotube, Figure 3B). The same line of reasoning can be applied to macrocycles **2**, where macrodipole-free dimers would bind anions weakly and then rotate to hand over the anion to the next dimer (Figure 7F). However, we repeat that the discussion of macrocycle **2** does not seem worthwhile because the activity profile is not very interesting.

Macrodipole−Potential Interactions. The Hill coefficients of **1** drop from $n = 4$ in unpolarized to $n = 1$ in polarized membranes (Figure 6A).[75−79] High Hill coefficients in unpolarized membranes demonstrated that the active suprastructure is at least tetrameric and thermodynamically unstable.[77−79] Decreasing Hill coefficients suggested that this active suprastructure is stabilized by increasing transmembrane membrane potentials. This unique behavior supported the existence of transmembrane parallel nanotubes as active suprastructures that are stabilized by macrodipole−potential interactions.

According to this interpretation, the dichotomic Hill coefficients of macrocycle **2** increase slightly with voltage because

their "antiparallel" dimers are destabilized by membrane potentials (Figures 6B, 7F, and S10). Inactivation with high gating charge $z_g = 0.54 \pm 0.08$ may thus originate from destructive macrodipole−potential interactions,[82] whereas reactivation at high voltage could indicate the enforced self-assembly into "parallel" nanotubes as with **1** (Figure 5D).

Ion Selectivity. The selectivity in transmembrane ion transport is arguably best described by the Eisenman theory[83] and its extension toward anions by Diamond and Wright.[84] This theory assumes that selectivity sequences depend on balancing the energy losses from dehydration and energy gains from binding to the anion binding site. In the Hofmeister series found for most simple anion transporters, selectivity is determined by the cost of dehydration only, demonstrating that anion binding by the transporter is weak.[1,31,32] Applied to **2** (Figure 3C), this was consistent with weak anion binding to two amide/urea donors at one face of an antiparallel dimer.

The dichotomic anti-Hofmeister behavior of macrocycle **1** demonstrated that anion binding by the active suprastructure is very strong, strong enough to overcompensate energy losses from at least partial dehydration (Figure 3D). Strong anion binding was in support of parallel nanotubes as active suprastructures. In this case, macrodipole−anion interactions can strengthen anion binding to four proximal H-bond donors at the positive end of the macrodipole to ultimately overcompensate energy losses from full or partial anion dehydration. The resulting active complex exists as an unstable minority system at nanomolar concentrations in an at least biphasic environment (see above).

Both macrocycles exhibit extra chloride selectivity beyond anti-/Hofmeister behavior. The molecular basis of this apparent chloride recognition is unknown. Control experiments disfavor experimental artifacts (e.g., Figure 3C); simple topological matching with the four preorganized H-bond donors at the positive end of the nanotube is a possibility that remains to be confirmed by computational studies.

The positive AMFEs obtained with macrocycle **2** probably originate from saturation with the better binding, "fast" anions and do not seem to be further noteworthy (Figure 4). However, saturation behavior can hardly account for the dichotomic negative AMFEs with **1**. Underadditive activity in mixtures of fast and slow anions is often viewed as support of cooperative multiion transport, that is, that the binding of more than one of the fast anions is needed to really move fast. Cooperative multiion transport is expected in the "Jacobs-ladder" mechanism for directional transport without macrodipole inversion (Figure 7D,E).

Taken together, this brief discussion suggests that the unusual behavior of macrocycle **1** originates from the macrodipole of the active nanotube and its interactions with anions and membrane potentials. The overall remarkably consistent set of experimental evidence should not distract from the fact that all interpretations made remain purely speculative. Voltage-sensitive Hill coefficients, concentration-dependent voltage-gating, anti-Hofmeister selectivity, negative AMFE, and so on naturally exist beyond any doubt as intriguing experimental facts. Their interpretation with operational parallel nanotubes, anion−macrodipole interactions, and molecular "Jacobs-ladder" toys may ultimately turn out to be right or wrong and is made with the only intention to stimulate discussion and progress of the field.

Conclusion

In conclusion, we have investigated the membrane transport properties of oligourea/amide macrocycles by various fluorescence-based assays. Aryl-substituted oligourea/amide macrocycles excel with high activity and variable anion selectivity reaching from simple Hofmeister to more attractive anti-Hofmeister behavior with additional chloride recognition. Binary mixtures of anions are transported with nonlinear mole-fraction behavior reaching from strongly positive to strongly negative AMFEs. Voltage sensitivity reaches gating charges up to 0.56 and is most pronounced for Hill coefficients. Taken together, these unusual characteristics suggest that oligourea/amide macrocycles self-assemble into parallel nanotubes and operate with macrodipole−potential and anion−macrodipole interactions. Whereas macrodipole−potential interactions have been considered previously in synthetic transport systems other than stacked macrocycles,[75−79] the use of anion−macrodipole interactions to achieve anion selective transport is unprecedented. The introduction of synthetic transporters that operate with new suprastructures, explore new ways to interact with ions, and employ new mechanisms for their transport is of highest interest, not only from a fundamental point of view but also with regard to future applications in medicinal and materials sciences.

Acknowledgment. We thank the Centre National de la recherche Scientifique (CNRS, GG), the Agence Nationale pour la Recherche (NT05442848, GG), the University of Geneva (SM), and the Swiss NSF (SM) for financial support.

Supporting Information Available: Experimental details. This material is available free of charge via the Internet at http://pubs.acs.org.

JA9067518

(82) Bainbridge, G.; Gokce, I.; Lakey, J. H. *FEBS Lett.* **1998**, *431*, 305–308.
(83) Eisenman, G.; Horn, R. *J. Membr. Biol.* **1983**, *76*, 197–225.
(84) Wright, E. M.; Diamond, J. M. *Physiol. Rev.* **1977**, *57*, 109–156.